

# Inverse Gas Chromatography, Surface Properties, and Interactions Among Components of Paint Formulations

A. Ziani, R. Xu, and H.P. Schreiber—CRASP\*  
T. Kobayashi—Nippon Paint Co.†

## INTRODUCTION

**T**hermodynamic interactions among components play a dominant role in the determination of properties in multi-component polymer systems, including those intended for use as protective coatings. Interactions have their origins at contacts among the system components and thus are closely related to the surface characteristics of these components. Recent publications have illustrated the close relationship between interactions and practical performance criteria of coating systems. Rheological behavior<sup>1</sup> and the stability of pigment dispersions<sup>2,3</sup> are among the criteria referred to. Therefore, a quantitative evaluation of surface properties and of component interactions is a desirable element in the knowledgeable formulation of coating systems.

Two principal contributions to component interactions are broadly recognized. One of these arises from Lifschitz-van der Waals (L/W), or universal dispersion forces, and is accessible from measurements such as the dispersion contribution to the surface energy of solids,  $\gamma_s^d$ . The other arises from non-dispersion forces and includes contributions from ionic, hydrogen-bond, covalent, polar, dipolar and similar interactions.<sup>4</sup> Following current convention, the totality of non-dispersion forces will be referred here to as acid-base (ab) forces. Although L/W forces act over larger distances than non-dispersion forces (by the Lennard-Jones potential model, L/W forces decay as the inverse 6th power, and non-dispersion forces as the inverse 12th power of the distance between interacting points), the latter make important contributions to the generation and the retention of properties related to interfacial phenomena, for example the strength of adhesive bonds between contacting materials. Quantitative measurement of non-dispersion, ab interactions, therefore, becomes a key facet of component characterization. The technique of inverse gas chromatography (IGC) has proven itself to be a convenient and powerful approach to this challenge. The subject of frequent descriptions and reviews,<sup>5-7</sup> IGC may be applied to measure aspects of surface energy, site

*Inverse gas chromatography (IGC) was applied to the surface characterization of polymers and pigments used in the formulation of protective coatings. IGC measurements over a significant temperature range provided surface energy and acid-base interaction parameters for these materials. Two sets of IGC data were obtained: (1) the quantity of vapor used to probe solid surfaces was extremely small, with results describing the properties of the most energetic surface sites; and (2) finite concentrations of vapor probes were used, with results describing the average properties of surface sites. A comparison of the two sets gave information on the heterogeneity of sites on the polymer and pigment surfaces. Heterogeneity parameters were defined for sites interacting through dispersion forces as well as for those able to interact as acids and bases. The present work reinforces the usefulness of surface characterizations by IGC by showing that the stability of pigments dispersed in the polymer vehicles was a function of the acid-base interaction between polymer-pigment pairs.*

\*Dept. of Chemical Engineering, Ecole Polytechnique, P.O. Box 6079, Stn. Centre Ville, Montreal, Que. H3C 3A7, Canada.

†19-17 Ikeda Nakamachi, Neyagawa, Osaka 572, Japan.

energy distribution, and thermodynamic interaction among the components of a polymer system. It has been used for each of these purposes in the present study, the first of a series dealing with interactions in coating systems and their relation to certain properties of the compounds. In the present case, we have used IGC to characterize the surface and interaction properties of three polymers and three pigments, all relevant to the formulation of coatings. Also reported are correlations with some practical aspects of coatings performance.

## EXPERIMENTAL

### Materials

The following polymers were used in this work. All were commercially produced resins supplied by Nippon Paint Co., Neyagawa, Japan.

NCSC—an acrylic copolymer consisting of styrene, n-butyl methacrylate, n-butyl acrylate, and maleic anhydride, with  $M_n = 3000$  and an acid value of 157.

HP—an acrylic copolymer of styrene, methyl methacrylate, n-butyl acrylate, 2-hydroxyethyl methacrylate, and glycidyl methacrylate, with  $M_n = 3000$  an epoxy value of 90, and OH value of 90.

ACR—an acrylic copolymer of styrene, ethyl acrylate, methyl methacrylate, ethyl methacrylate 2-hydroxyethyl methacrylate, and methacrylic acid, with  $M_n = 21,000$  an acid value of 15, and OH value of 45.

The opacifiers used were:

R—a rutile  $TiO_2$  pigment, surface-coated by the manufacturer with alumina and zirconia, with a (BET) specific surface area of  $11.9 \text{ m}^2/\text{g}$  and a density of  $4.11 \text{ g/ml}$ .

BP—a bare diketo-pyrrolo-pyrol red pigment, with a specific surface area of  $29.0 \text{ m}^2/\text{g}$  and a density of  $1.6 \text{ g/ml}$ .

BL—a commercially surface coated version of BP, with a specific surface area of  $31.0 \text{ m}^2/\text{g}$ , and a density of  $1.6 \text{ g/ml}$ . The coating composition has not been disclosed.

### Procedures

**IGC AT EXTREMELY LOW PROBE CONCENTRATION:** IGC was used for the surface characterization of the experi-

mental materials. At first, the conventional procedure was used based on the injection of vapor probes at extreme dilution. To prepare stationary phases of the polymers for IGC, these were coated onto Chromosorb A/W, 60/80 mesh support from 5 wt% solutions using 1:1 mixtures of p-xylene and ethylethoxypropionate as solvents. Ashing analysis showed that the supported mass of polymer fell in the range 7.2–8.8 wt%, sufficient to ensure full coverage of the available support surface. Coated, carefully dried supports were then packed in previously degreased, washed, and dried stainless steel columns, 4 mm in diameter and generally 45–50 cm in length. Pigments were packed directly into stainless steel columns, 2.4 mm in diameter and 20–35 cm long. The mass of retained pigment was 0.377 g for R, 0.616 and 0.702 g for BL and BP, respectively. A Varian 3400 gas chromatograph equipped with ionizing flame and hot wire detectors was used throughout the work. The temperature range covered was from  $30^\circ\text{C}$ – $60^\circ\text{C}$  for the polymers and  $30^\circ\text{C}$ – $80^\circ\text{C}$  for the pigments. Prior to data collection all materials were conditioned at  $110^\circ\text{C}$  under a flow of He carrier gas. A soap bubble flowmeter was used to control the flow rate of He, in most cases at  $15 \text{ mL/min}$ .

The vapor probes used to study surfaces of the stationary phases were the n-alkanes from C6–C10. Polar probes were diethyl ether (DEE), chloroform (CHL), ethyl acetate (EAc), tetrahydrofuran (THF), dichloromethane (DCM), and acetone (AC). The latter group was chosen on the basis of Gutmann's theory of acids and bases, which assigns electron acceptor (acid) and donor (base) numbers, AN and DN to them. However, in Gutmann's original tabulations<sup>8</sup> only DN has conventional thermodynamic units, AN being based on facets of NMR spectroscopy. This results in asymmetry between the units of parameters. The problem was resolved by taking into account the L/W contribution to AN, as proposed by Riddle and Fowkes.<sup>9</sup> The corrected parameter,  $AN^*$ , then has the same units as DN, namely kcal/mol. In the first series of experiments, the vapors were injected at very low concentration, achieved by 10 times voiding in air a  $10 \mu\text{L}$  Hamilton syringe initially filled with liquid probe. The quantity of vapor injected by the procedure was about  $2.4 \times 10^{-4} \mu\text{mol}$ . Each probe was injected in at least triplicate, with retention times repeatable to within  $\pm 4\%$ . Retention volumes,  $V_n$ , calculated from retention times by well known procedures<sup>5,6</sup> had similar exper-

imental uncertainties. Dispersion surface energies of the solids were obtained from fundamental equations linking  $V_n$  with thermodynamic interaction parameters. The equations are due to Gray,<sup>10</sup> Papirer,<sup>11</sup> Schultz,<sup>12</sup> and their co-workers. A useful form is the statement:

$$RT \ln V_n = 2 N a (\gamma_i^d)^{1/2} (\gamma_s^d)^{1/2} + C \quad (1)$$

Where  $a$  is the cross-sectional area of the adsorbed vapor molecule (see Table 1), the  $\gamma$  are dispersion surface energies of the vapor in the liquid state and the stationary phase solid (sub-

**Table 1—Dimensions, Acid ( $AN^*$ ), and Base (DN) Interaction Characteristics of Vapors Used as Probes in IGC**

Vapor Probe:	$a \text{ (Å}^2\text{)}$	$AN^*$	DN	DN/ $AN^*$
Dichloromethane (DCM) .....	40	3.9	0	0
Chloroform (CHL) .....	44	5.4	0	0
Acetone (AC) .....	42.5	2.5	17.0	6.8
Ethyl acetate (EAc) .....	48	1.5	17.1	11.4
Tetrahydrofuran (THF) .....	45	0.5	20.0	40.0
Diethyl ether (DEE) .....	47	1.4	19.2	13.7
n-Hexane .....	51.5	—	—	—
n-Heptane .....	57	—	—	—
n-Octane .....	62.8	—	—	—
n-Nonane .....	68.9	—	—	—
n-Decane .....	75.2	—	—	—

scripts *l* and *s* respectively), *C* is an integration constant dependent on the selected reference state of the vapors, *N* is Avogadro's number, *R* is the gas constant, and *T* is the temperature in °K. Since alkanes are able to interact with the solids only through *L/W* forces, a plot of  $RT \ln V_n$  versus  $a(\gamma_1^d)^{1/2}$  for these vapors yields a reference straight line, from which may be obtained ( $\gamma_s^d$ ). If the solid under investigation can act as acid and/or base, then the retention volumes for polar probes will be greater than those of corresponding alkanes of the same dimension and it follows<sup>10-12</sup> that

$$RT \ln V_n/V_n^{\text{ref}} = -\Delta G^{\text{ab}} \quad (2)$$

Where  $V_n^{\text{ref}}$  is the retention volume of the relevant alkane probe and  $\Delta G^{\text{ab}}$  is the acid-base contribution to the free energy of desorption of the polar probe. When this datum is measured over an appropriate temperature range, the acid-base contribution to the desorption enthalpy follows from the relationship:

$$\Delta G^{\text{ab}} = \Delta H^{\text{ab}} - T\Delta S^{\text{ab}} \quad (3)$$

Assuming  $AN^*$  and  $DN$  for the probes are known, the acid-base interaction parameters *K<sub>a</sub>*, *K<sub>d</sub>* for the solids under study may be evaluated by plotting  $\Delta H^{\text{ab}}/AN^*$  versus  $DN/AN^*$ , as prescribed by

$$\Delta H^{\text{ab}}/AN^* = K_a(DN/AN^*) + K_d \quad (4)$$

Finally, once *K<sub>a</sub>* and *K<sub>d</sub>* values have been measured for components of a polymer system, it is possible to evaluate an acid-base pair interaction parameter *I<sub>sp</sub>* from

$$I_{\text{sp}} = (K_a)_1(K_d)_2 + (K_a)_2(K_a)_1 - (K_a)_1(K_a)_2 - (K_d)_1(K_d)_2 \quad (5)$$

The reason for subtracting like-like interactions from the unlike acid-base contributions has been discussed earlier.<sup>15</sup> The route to interaction and surface energy data described earlier depends on knowledge of the parameter *a*. The dimensions of many organic molecules have been tabled in the literature and are reproduced in Table 1. The applicability of these data to the IGC approach is, however, open to some question since the molecule may be perturbed when adsorbed on a surface. Molecular distortion would be particularly noticeable at low injection volumes where the distance between surface and adsorbing molecules is minimized. Also, since IGC data can be collected over a wide temperature range, it is appropriate to take into account the temperature dependence of molecular dimensions. Density-temperature relationships are a convenient route to this correction;<sup>16,17</sup> however, difficulties associated with the use of parameter *a* may be reduced appreciably by substituting for it with either the saturation vapor pressure of the probe (at the relevant temperature), or its normal boiling temperature. It has been shown<sup>18</sup> that nearly identical values of dispersion surface energy, of enthalpy and of *K<sub>a</sub>*, *K<sub>d</sub>* parameters are obtained with any of the three options for data representation.

**FINITE CONCENTRATION IGC:** An important aspect of solid surfaces is their heterogeneity. In inorganic and organic solids, surface heterogeneity may arise from inclusions of impurities, morphological effects, and edge and corner effects, etc. In polymers, molecular weight

variations and structural differences between surface and bulk can contribute to surface irregularities. These may influence adsorption, adhesion, and related properties of the polymers, making desirable an evaluation of the degree of heterogeneity. In the great majority of solids, the heterogeneity may be viewed as a distribution of surface site energies.<sup>3,13,14</sup> At very high dilution of injected vapor probes in the IGC method, thermodynamics dictate that the retention data will characterize sites of the highest surface energy. Only at higher concentrations of injected probes will these occupy greater fractions of the accessible surface sites, eventually characterizing sites of average energy. In this work, a partial scan was made of site energy variations by injecting vapors at finite concentration. By reducing the number of times that initially filled microsyringes were voided, the injected quantity of vapor could be increased systematically to a maximum of  $2500 \times 10^{-4}$   $\mu\text{L}$ . Provided the linearity prescribed by equation (1) holds when alkanes are injected at finite concentration,  $\gamma_s^d$  may be used as a measure of the energy variations in sites interacting by *L/W* forces. Similarly, the  $\Delta G$  for selected acid and base probes injected at finite concentrations may be used as an index of energy variations in surface sites acting as electron donors and acceptors.

**CONTACT ANGLE ANALYSIS:** Static contact angle (c.a.) measurements were made for comparisons of surface energies with the IGC results. Unlike IGC, in which a very small number of molecules probes a large surface area, in c.a. work a relatively large droplet of probe liquid contacts a small surface area. Thus, the c.a. datum corresponds to a measurement of an average surface energy, and expectedly will be lower than data obtained by the extremely dilute IGC approach. The difference between the two results may be used as a rough indication of surface heterogeneity on dispersion-force sites. Of course, an added advantage of c.a. measurements is the evaluation of the non-dispersion, or acid-base contribution to surface energy,  $\gamma_s^{\text{ab}}$ , a datum not readily obtained from IGC. This assumes that the division of the measured total surface energy into its constituent parts, as suggested by Fowkes,<sup>19</sup> Good,<sup>20</sup> and their co-workers, among others, is valid. Contact angles were measured on polymer samples only. Specimens were prepared by immersing freshly cleaned and dried microscope slide glass into approximately 3 wt% solutions of the polymers, and drying under a slow stream of nitrogen at 40°-45°C for about three hours, followed by 24-hr exposure in a vacuum oven at 60°C. Vacuum oven treatment was continued for at least four hours following attainment of constant weight. A modified Rame-Hart goniometer was used for c.a. measurements. The polymer sample was placed on the thermostated stage of the goniometer at 22°C, and enclosed in a glass dome, as described earlier.<sup>21</sup> A 10  $\mu\text{L}$  syringe was used to deposit onto the polymer surface droplets of test liquids which included *n*-decane, tricresyl phosphate, formamide, glycerol, and water. In each case an open vial of the test fluid was placed into the enclosed goniometer space, so as to saturate that space with respect to the fluid's vapor, and to prevent evaporation of the test droplet. Readings of the c.a. ( $\theta$ ) were taken at 10 sec intervals for the first minute of contact and then every 60 sec for an additional 15-min

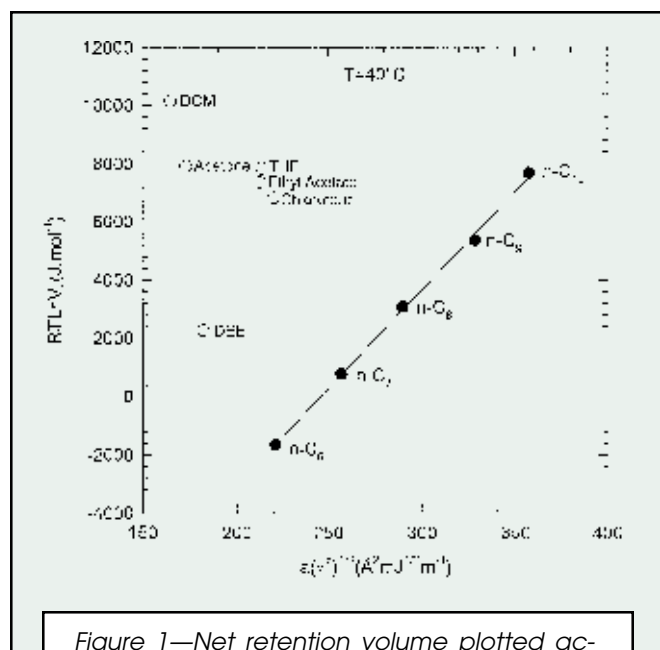


Figure 1—Net retention volume plotted according to equation (1) as a function of molecular parameters for adsorbed probes. Solid is polymer NCSC.

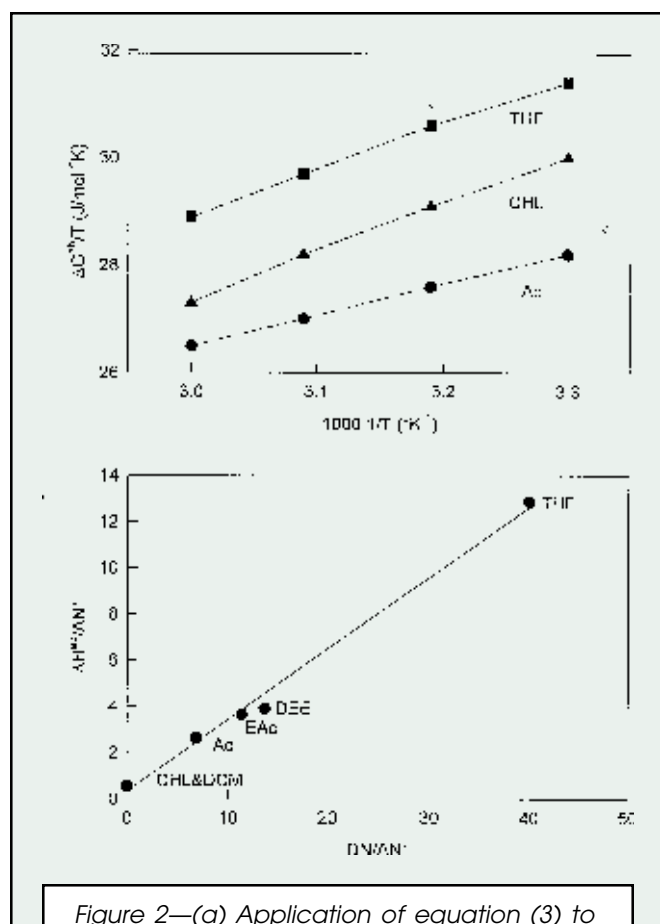


Figure 2—(a) Application of equation (3) to evaluate enthalpies of adsorption on NCSC polymer; (b) application of equation (4) to obtain acid-base interaction constants on polymer NCSC.

period. Following previously described procedures,<sup>15</sup> c.a. data were extrapolated to zero contact time, and the extrapolated value of  $\theta$  was used for calculations of  $\gamma_s^d$  and  $\gamma_s^{ab}$ , using the harmonic mean equations:

$$(1 + \cos \theta_1)\gamma_1 = 4 [(\gamma_1^d \gamma_s^d / \gamma_1^d + \gamma_s^d) + (\gamma_1^{ab} \gamma_s^{ab} / \gamma_1^{ab} + \gamma_s^{ab})] \quad (6)$$

and

$$(1 + \cos \theta_2)\gamma_2 = 4 [(\gamma_2^d \gamma_s^d / \gamma_2^d + \gamma_s^d) + (\gamma_2^{ab} \gamma_s^{ab} / \gamma_2^{ab} + \gamma_s^{ab})]$$

Here the subscripts 1 and 2 relate to liquids 1 and 2, for which both  $\gamma^d$  and  $\gamma^{ab}$  (i.e.,  $\gamma^{nd}$ ) are known. In this work formamide and water were the chosen fluids. Simultaneous solution of the equations then leads to the wanted numbers for the solid,  $s$ .

**STABILITY OF PIGMENT DISPERSION:** A critical aspect of paint technology is the stability of pigment dispersions in polymer vehicles. Dispersion stability was chosen as a practical criterion against which to assess the usefulness of the surface energy and interaction analyses. The procedure followed in the set of nine systems was as follows: Stock solutions containing 1 wt% of each polymer were prepared for use as dispersion vehicles. To 50 mL aliquots of these, placed in an Erlenmeyer flask, were added 3 g of pigment, and the solids were dispersed by agitating with a magnetic stirrer for 24 hr. Following this step, 10 mL quantities of the dispersions were poured into graduated centrifuge tubes, and the solids were allowed to settle for up to 16 hr. Periodic readings were taken of the volume of clarified supernatant liquid. At least three samples were analyzed from each dispersion. Finally, each system was centrifuged and an equilibrium value of clarified liquid volume (or sedimentation volume) was determined. Plots of clear volume versus time allowed for the specification of a comparison parameter,  $t_{1/2}$ , representing the time required for 50% of the final clarified volume to be attained.

## RESULTS AND DISCUSSION

**IGC CHARACTERIZATION—PROBE INJECTION AT VERY LOW CONCENTRATION:** An important first step in the use of IGC for surface characterization is to make certain that the linearity called for by equation (1) is observed. The data in Figure 1 for NCSC polymer at 40°C are typical of results obtained for all the stationary phases of this work. Clearly, when alkane vapors are injected, the expected linearity is met. The slope of the line then provides a value of  $\gamma_s^d$  for high energy sites in the polymer surface. The position of polar probes falls above the reference line defined by the alkanes, indicating that the polymer is able to interact with both acidic and basic probes. The AN\* and DN values of the polar probes have been entered in Table 1. They classify THF and DEE as strong bases, CHL and DCM as strong acids, and Ac and EAc as relatively well balanced or amphoteric probes. Since acidic, basic, and amphoteric probes fall above the reference line defined by alkane vapors in Figure 1, the polymer has surface sites able to act as electron donors and electron acceptors. Figure 2 illustrates the procedure leading to other valuable interaction parameters. Figure 2a, shows the embodiment of equation (3), the slope of the well-defined line giving the value of  $\Delta H^{ab}$  for each of the

Table 2—Summary of Surface Interaction Characteristics, from IGC and Contact Angle Analysis

	$(\gamma_s^d)_{IGC}^*$ -- (mJ/m <sup>2</sup> ) --	$(\gamma_s^d)_{c.a.}$ --	Ka	Kd	Ka/Kd	Ka+Kd
<b>Pigments</b>						
R .....	57.7	—	5.9	3.3	1.78	9.2
BL .....	38.2	—	0.15	0.98	0.15	1.1
BP .....	47.9	—	0.20	0.60	0.35	0.8
<b>Polymers</b>						
NCSC .....	33.5	30.2	0.56	0.29	1.93	0.8 <sub>5</sub>
HP .....	31.7	30.0	0.62	0.46	1.34	1.1
ACR .....	34.4	32.5	0.40	0.29	1.38	0.7
<b>Pair interaction parameters values, Isp:</b>						
R/NCSC = -0.7		BL/NCSC = 0.23		BP/NCSC = 0.12		
R/HP = -0.2		BL/HP = 0.14		BP/HP = 0.06		
R/ACR = -0.4		BL/ACR = 0.10		BP/ACR = 0.05		

probes used in the experiment (to avoid overcrowding only one alkane an acid and a base probe are shown). Figure 2b applies equation (4) using the measured adsorption enthalpies for each of the polar probes to obtain the Ka and Kd constants for the NCSC polymer. The interaction parameters may be considered valid over the 30° range of the IGC study. The relative positions of lines in Figure 2a indicates a slight predominance of acidic surface characteristics in this polymer. The matter is substantiated in Figure 2b which reports Ka = 0.56 and Kd = 0.29. Clearly, the surface arrangement of polymer chains favors the prevalence of adsorption sites acting as electron acceptors. The likely source of these is the maleic anhydride moiety.

Analogous steps to those discussed previously have resulted in a compilation of surface interaction characteristics for all of the materials in this study. The data are presented in Table 2. High energy dispersion sites in the polymers are similar, although those in ACR are marginally higher and those in HP somewhat lower than the mean. All fall well below the values for the pigments, indicating that dispersion forces will favor wetting of the pigments by the polymers. The coated rutile has by far the most energetic of the dispersion-force sites. The comparison between  $\gamma^d$  from IGC and c.a. measurements suggests a narrow, 5-10% range of variations in the dispersion site energies of these polymer surfaces. The site heterogeneity is examined in more detail in the next section. The rutile pigment and all three of the polymers are net acids, with Ka/Kd > 1, while the organic solids BL and BP are net bases. Thus, significant acid-base interaction may be expected to contribute to bond strength at interfaces between the polymers BL or BP. The strength of interfaces with R, however, will depend on the effectiveness of dispersion forces in overcoming the unfavorable short-range interactions. A quantitative restatement of these observations is in the values of the pair interaction parameter, Isp, also entered in Table 2. Negative entries for each of the systems involving R signals the absence of acid-base interfacial forces, the lack being most pronounced in the pair R/NCSC. Positive acid/base interactions are noted with the two organic pigments, those with BL somewhat exceeding their counterparts with BP. Evidently, the applied surface coating is effective in improving the adhesion between polymer

vehicles and the organo-red pigment. Finally, a rough estimate of total acid-base interactivity (per unit of surface area) may be obtained by summing Ka and Kd. By this convention the most interactive solid is the rutile, others tending to fall in the range of 1.0. The exception is polymer ACR, where acid-base functionality is somewhat weaker.

**FINITE CONCENTRATION IGC:** A significant added aspect of surface characterization of solids involved in coatings formulations is the ability of IGC to provide a measure of the site energy heterogeneity in these materials. This may be done by determining  $\gamma^d$ ,  $\Delta G^a$ , and  $\Delta G^b$  (respectively the individual acid and base contributions to the free energy of desorption) at finite concentrations of the injected vapors. A prerequisite to computing  $\gamma^d$  values from IGC results at finite concentrations of injected probes is the continued applicability of equation

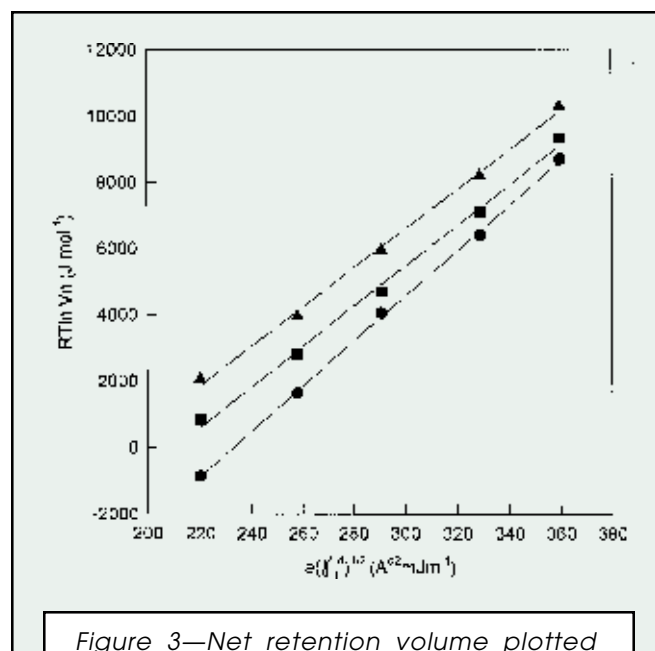
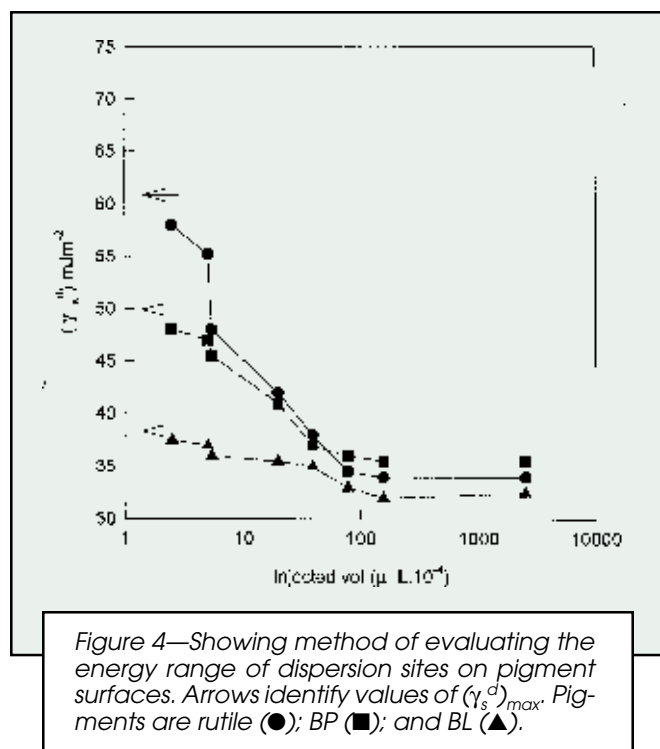


Figure 3—Net retention volume plotted against molecular parameters for various volumes of probe injection. Solid is polymer NCSC at 35°C: Injection volumes are  $2.44 \cdot 10^{-4} \mu\text{L}$  (●);  $39.1 \cdot 10^{-4} \mu\text{L}$  (■); and  $2500 \cdot 10^{-4} \mu\text{L}$  (▲).





(1), as confirmed by the linearity of plots of  $RT \ln V_n$  versus  $a(\gamma_1^d)^{1/2}$ . Fortunately, in all of the present materials, linearity was maintained. An illustration is given in Figure 3 for polymer NCSC at 35°C. For clarity, only three injection volumes are shown, including the maximum in this work of  $2,500 \cdot 10^{-4} \mu\text{L}$ . Dispersion surface energies, therefore, may be calculated over an appreciable range of injection volumes. Further, the placement of polar probes relative to the alkane reference at each of the injection volumes allows an evaluation to be made of  $\Delta G^{ab}$ . It is convenient to choose a reference acidic and basic probe to obtain values of  $\Delta G^a$  and  $\Delta G^b$  individually. An arbitrary selection was made for THF as the basic reference, providing values of the  $\Delta G^a$  parameter, while the heterogeneity in basic surface sites was monitored with DCM as the acidic reference probe.

Of course, the quantity of probe injected at maximum dilution ( $2.44 \cdot 10^{-4} \mu\text{L}$ ) still represents a significant number of molecules associating with the available solid

surface. Thus, the surface energy and free energy parameters measured in the extreme dilution experiment do not necessarily correspond to maximum values of the parameter for the solid in question. To estimate the maximum quantity, it is necessary to establish the relationship between the desired parameter and the injection volume. The procedure is illustrated in Figure 4, with  $\gamma_s^d$  of the three pigments as the parameter of concern. The extrapolation to  $10^{-4} \mu\text{L}$  of probe injection is defined as a reference point for the specification of  $(\gamma_s^d)_{\max}$ , while the plateau datum at greatest injection volumes identifies  $(\gamma_s^d)_{\min}$ . Similar procedures were used to obtain  $(\Delta G^a)_{\max}$ ,  $(\Delta G^b)_{\max}$ , and the corresponding minima. The  $\Delta G$  values refer to the retention volumes of the reference acid and base probes. Thus,  $\Delta G^a$  characterizes the basic sites of the solid surface, and  $\Delta G^b$  the acidic sites. Site heterogeneity indexes (SH) may then be defined as follows:

$$(\text{SH})^d = (\gamma_s^d)_{\max} / (\gamma_s^d)_{\min}$$

$$(\text{SH})^b = (\Delta G^a)_{\max} / (\Delta G^a)_{\min} \quad (7)$$

$$(\text{SH})^a = (\Delta G^b)_{\max} / (\Delta G^b)_{\min}$$

The results are summarized in Table 3. For the three polymers, the measurement of  $\gamma^{ab}$  ranks the contribution of non-dispersion forces to the total surface energy in the order  $\text{HP} > \text{NCSC} > \text{ACR}$ . This corresponds to the order in their total specific interaction potential ( $K_a + K_d$ ) seen in Table 2. Notable in Table 3 is the excellent agreement between the polymer  $\gamma^d$  values from c.a. measurements and from IGC evaluations at maximum probe volume injection. The inorganic R pigment has by far the largest absolute values of site energy parameters. The sites interacting with L/W forces also have the largest variation in the set. Of the two organic pigments, the coated version, BL, has consistently greater site homogeneity than does the bare version of this pigment. The dispersion site energy distribution for the three polymers is constant, the variation from maximum to minimum values lies in the 10% range. Much bigger variations are recorded for sites acting as acids and bases. In this category the site energy distribution for the three polymers appears to be considerably wider than in the pigments; however, the relatively larger uncertainty of determinations when  $\Delta G \leq 1$  may be contributing to these apparently high values of the SH index. Notable also is a tendency for wider distributions in the energies

Table 3—Surface Site Heterogeneity Parameters, Surface Energy and Free Energy Variations from Which They are Calculated

Material	R	BL	BP	NCSC	HP	ACR
<b>Parameter:</b>						
$(\gamma_s^d)_{\max} (\text{mJ/m}^2)$ .....	61	38.5	49.5	34.0	32.5	35.5
$(\gamma_s^d)_{\min} (\text{mJ/m}^2)$ .....	34	32.5	36.0	29.8	29.5	32.0
$(\gamma_s^d)_{\text{c.a.}} (\text{mJ/m}^2)$ .....	—	—	—	30.2	30.0	32.5
$(\gamma^{ab})_{\text{c.a.}}$ .....	—	—	—	4.0	4.4	3.5
$(\text{SH})\gamma^d$ .....	1.8	1.2	1.4	1.1	1.1	1.1
$(\Delta G^a)_{\max}$ .....	19.0	1.0	1.7	4.4	4.6	4.0
$(\Delta G^a)_{\min}$ .....	13.5	0.2	0.3	0.7	1.0	0.5
$(\text{SH})^b$ .....	1.4	5.0	5.7	6.3	4.6	8.0
$(\Delta G^b)_{\max}$ .....	12.0	3.3	2.9	3.3	3.9	3.5
$(\Delta G^b)_{\min}$ .....	6.0	2.4	1.6	0.4	0.8	0.6
$(\text{SH})^a$ .....	2.0	1.4	1.8	8.2	4.9	5.8

of dominant sites. Thus, in the strongly acidic coated rutile, the breadth of energy variations in acidic sites (about 100%) is distinctly greater than the 40% variation in basic site energies. Similar remarks may be made for polymers NCSC and ACR. The reverse is evident in the basic organic solids BL and BP. At the present no cause can be offered for this observation.

**PIGMENT DISPERSION STABILITY:** Our objective here was to show whether or not the interaction at pigment/polymer interfaces, as quantified by the  $I_{sp}$  parameter, could rationalize the stability of pigment dispersions in the systems under present consideration. Therefore, a link was sought between the thermodynamics-based surface interaction criteria and practical aspects of paint technology. The dispersion stability descriptor  $t_{1/2}$  was obtained from plots such as that of Figure 5, showing the sedimentation process in dispersions of BP pigment in the NCSC and HP vehicles. In both cases a well-defined plateau value allows for the definition of the  $t_{1/2}$  parameter to within  $\pm 15$  min. Evidently, polymer NCSC is a more successful stabilizer for this pigment than is HP. An overall view of the relation between  $t_{1/2}$  and  $I_{sp}$  is given in Figure 6. There is a strong indication that dispersion stability increases with increasing degree of acid-base interaction at the pigment/polymer interface. This extends similar findings reported in reference (1), but the result must be viewed with some reservations. The reason for this is that the behavior of the pigment dispersion is the result of an interaction balance also involving the polymer/solvent and the pigment/solvent interfaces. These competitive interactions could exert an appreciable effect on the tendency of the polymer to adsorb from solution and on the configuration of the adsorbed

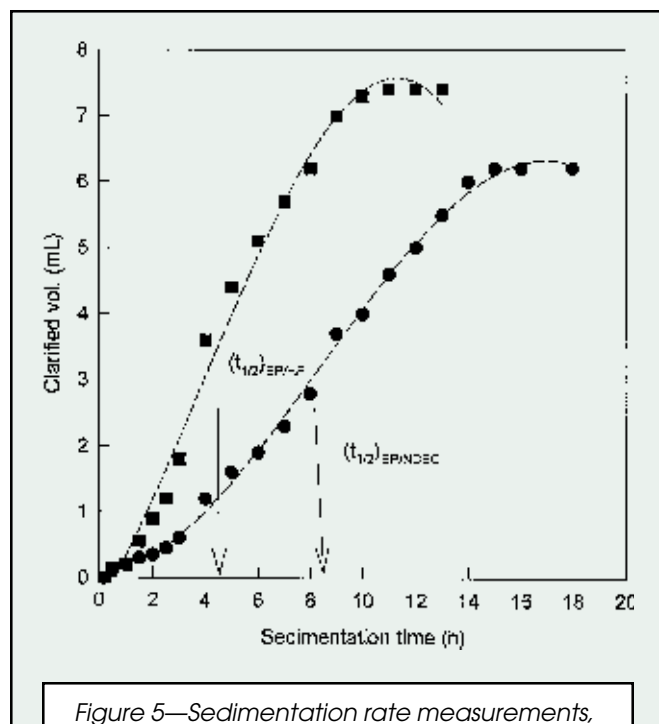


Figure 5—Sedimentation rate measurements, showing definition of  $t_{1/2}$  parameter, for BP pigment dispersions in BP and NCSC polymer vehicles.

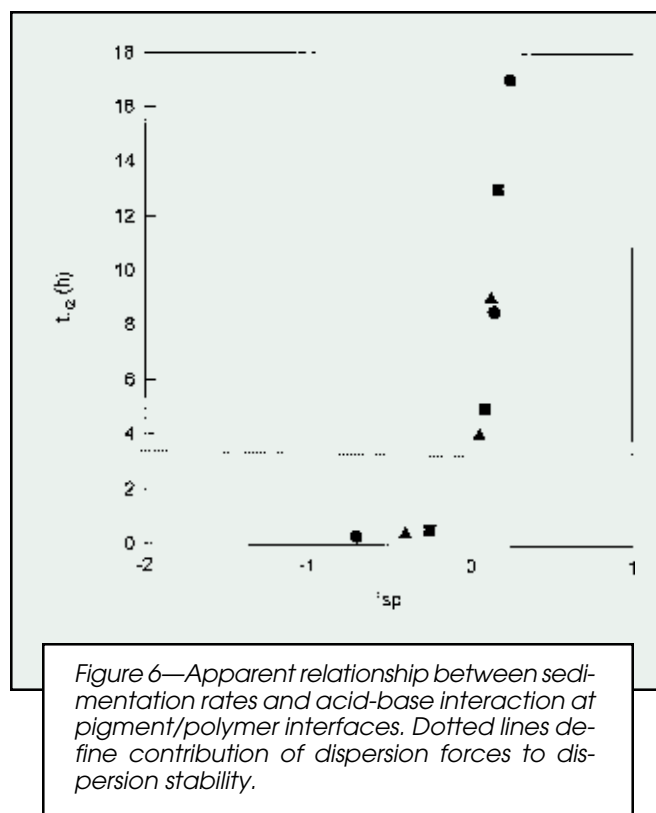


Figure 6—Apparent relationship between sedimentation rates and acid-base interaction at pigment/polymer interfaces. Dotted lines define contribution of dispersion forces to dispersion stability.

molecules. Both of these factors could in turn influence the stability of the dispersed phase. Polymer/solvent and pigment/solvent interactions may be accounted for by parameters such as the Flory  $\chi$  value,<sup>22</sup> which is accessible, in principle, from IGC measurements.<sup>5</sup> In this work, however, the necessary and tedious procedures were not followed. Another possible limitation to the situation displayed in the figure is due to the comparison among the systems being made at varying degrees of surface coverage. This is the consequence of using the same mass of pigment per unit volume of polymer solution, even though the surface areas of the three solids are not equivalent. On the other hand, the amount of polymer available was in excess of that required to form a monolayer on the available surface thereby reducing the impact of this effect. Attention also is drawn to the linear portion in Figure 6. This cannot be expected to continue indefinitely with corresponding benefits to dispersion stability. Dispersion stability in non-aqueous systems is closely related to the concept of steric or entropic stabilization.<sup>3,23</sup> According to this, the stability of dispersions relies on a non-permissible loss of entropy, when two solid particles with adsorbed polymer come into close proximity. If at low or negative  $I_{sp}$  the mass of adsorbed polymer is not sufficient, inadequately covered pigment particles can agglomerate on collision, eventually settling from solution. This process accounts for the tailing-off of the relation near  $I_{sp} = 0$ . At intermediate degrees of pigment/polymer interaction, the adsorbed polymer still extends sufficiently into the solvent to create the entropic block to effective particle collision. However, at high values of  $I_{sp}$ , in these cases evidently at  $I_{sp} \geq 1$  and not attained by any of the systems studied, the polymer becomes too closely held on the solid surface. The net

result is an effective increase in the pigment particle diameter, but there is an inadequate protective layer of swollen polymer around the particle. The entropic barrier is reduced and settling of solids will again accelerate. Thus, only the part leading toward a maximum in the expected relationship has been traced out by the systems of this work. Finally, in Figure 6, attention is drawn to the dotted line construction, which assigns a  $t_{1/2}$  value near 3.5 hr to the stabilizing effect of L/W dispersion forces at the pigment/polymer interface. It is interesting that the  $t_{1/2}$  data for systems with negative  $I_{sp}$ , all associated with the rutile pigment, fall below that line. Steric considerations hindering the approach of polymer segments into sufficient proximity of the solid to bring L/W forces into full play may be responsible. The existence of like-like pairings (effectively acid-acid repulsion) at these interfaces also may contribute to the observation. Additional systems will need to be studied in order to resolve the questions raised by these results. However, the fundamental importance of acid-base interactions and their significance to the practical performance of coatings formulations is not to be doubted.

## CONCLUSIONS

IGC analysis at very high dilution and at finite concentration of probe injection has been carried out on a series of polymers and pigments used in paint formulations. Values of dispersion surface energies, and of acid-base interaction parameters have been obtained for the materials, and pair interaction parameters calculated from the results.

IGC data at very dilute probe concentration have characterized the surface energies and acid-base interaction potentials of the high energy sites in the material surfaces. At high concentration of injected probes, the corresponding average properties of surface sites have been evaluated. The ratio of the two sets of values has been used to estimate the site energy distribution in the polymers and pigments.

The dispersion stability of each pigment/polymer combination has been measured and correlated with the acid-base interaction parameters of the materials. The correlation is strong, justifying the availability of fundamental thermodynamic interaction data to optimize performance aspects of protective coatings.

The data in hand are sufficient to define only a portion of a more complex relationship between dispersion stability and acid-base forces at polymer/pigment interfaces. A broader study is called for to define the relationship in greater detail.

## ACKNOWLEDGMENT

The Natural Sciences and Engineering Council, Canada is gratefully acknowledged for their financial support of this research. Additional support was received from Nippon Paint Co., to whom thanks also are expressed for permission to publish.

## References

- (1) Lara, J.A. and Schreiber, H.P., *J. Polymer Sci. Phys. Ed.*, **34**, 1733 (1996).
- (2) Creutz, S., Jerome, R., Kaptijn, G.M.P., van der Werf, A.W., and Akkerman, J.M., "Design of Polymeric Dispersants for Waterborne Coatings," *JOURNAL OF COATINGS TECHNOLOGY*, **70**, No. 883, 41 (1998).
- (3) Mukhopadhyay, P., Desbaumes, L., Schreiber, H.P., Hor, Ah-Me, and Baranyi, G., *J. Appl. Polymer Sci.*, **67**, 245 (1997).
- (4) Wu, S., *Polymer Interfaces and Adhesion*, Ch. 1, Marcel Dekker Inc., New York, 1982.
- (5) Lloyd, D.R., Ward, T.C., and Schreiber, H.P., *Inverse Gas Chromatography*, ACS Symposium Series, 391, American Chemical Society, Washington, D.C., 1989.
- (6) Hegedus, C.R. and Kamel, I.L., "A Review of Inverse Gas Chromatography Theory Used in the Thermodynamic Analysis of Pigment and Polymer Surfaces," *JOURNAL OF COATINGS TECHNOLOGY*, **65**, No. 820, 23 (1993).
- (7) Hegedus, C.R. and Kamel, I.L., "Thermodynamic Analysis of Pigment and Polymer Surfaces Using Inverse Gas Chromatography," *JOURNAL OF COATINGS TECHNOLOGY*, **65**, No. 820, 31 (1993).
- (8) Gutmann, V., *The Donor-Acceptor Approach to Molecular Interactions*, Ch. 2, Plenum Press, New York, 1978.
- (9) Riddle, F.L. Jr. and Fowkes, F.M., *J. Amer. Chem. Soc.*, **112**, 3250 (1990).
- (10) Gray, D.G. and Dorris, G.M., *J. Colloid Interf. Sci.*, **77**, 353 (1980).
- (11) St. Flour, C. and Papirer, E., *J. Colloid Interf. Sci.*, **91**, 63 (1983).
- (12) Schultz, J. and Lavielle, M., in *Inverse Gas Chromatography*, Lloyd, D.R., Ward, T.C., and Schreiber, H.P. (Eds.), ACS Symposium Series, 391, Ch. 14, American Chemical Society, Washington, D.C., 1989.
- (13) Wesson, S.P. and Allred, R.E., *J. Adhesion Sci. Technol.*, **4**, 277 (1990).
- (14) Ballard, H., *Langmuir*, **13**, 1260 (1997).
- (15) Kloubek, J. and Schreiber, H.P., *J. Adhesion*, **42**, 87 (1993).
- (16) Dong, S., Brendle, M., and Donnet, J.-B., *J. Chim. Phys.*, **88**, 1831 (1991).
- (17) Mukhopadhyay, P. and Schreiber, H.P., *J. Polymer Sci., Phys. Ed.*, **32**, 1653 (1994).
- (18) Panzer, U. and Schreiber, H.P., *Macromolecules*, **25**, 3633 (1992).
- (19) Fowkes, F.M., *Ind. Eng. Chem.*, **56**, 40 (1964).
- (20) Girifalco, L.A. and Good, R.J., *J. Phys. Chem.*, **61**, 904 (1957).
- (21) Carre, A., Gamet, D., Schultz, J., and Schreiber, H.P., *J. Macromol. Sci., Chem.*, **A-23**, 1 (1986).
- (22) Flory, P.J., *Principles of Polymer Chemistry*, Cornell University Press, Ithaca, NY, 1953.
- (23) Napper, D.H., *Polymeric Stabilization of Colloidal Dispersions*, Academic Press, New York, 1983.